Research Square

Preprints are preliminary reports that have not undergone peer review.
They should not be considered conclusive, used to inform clinical practice,
or referenced by the media as validated information.

Global patterns of poaching probability in terrestrial mammals

Martina Fernando

martina.fernando@uniroma1.it

Department of Biology and Biotechnology, Sapienza University of Rome

Ana Benítez López

Museo Nacional de Ciencias Naturales (MNCN-CSIC) https://orcid.org/0000-0002-6432-1837

Marco Davoli

Department of Biology and Biotechnology, Sapienza University of Rome

Martin Philippe-Lesaffre

Department of Biogeography and Global Change, Museo Nacional de Ciencias Naturales (MNCN-CSIC), Madrid, Spain

Michela Pacifici

Department of Biology and Biotechnology, Sapienza University of Rome https://orcid.org/0000-0002-4468-4710

Article

Keywords:

Posted Date: October 5th, 2026

DOI: https://doi.org/10.21203/rs.3.rs-11231325/v1

License: This work is licensed under a Creative Commons Attribution 4.0 International License.
Read Full License

Additional Declarations: There is **NO** Competing Interest.

Title: Global patterns of poaching probability in terrestrial mammals

Abstract

Sustainable wildlife harvest is crucial for ensuring ecological balance while maintaining healthy population offtake levels in the long term. Yet a substantial share of hunting is illegal and spatially undocumented, risking declines that pass unnoticed until recovery is no longer possible. Existing threat maps rarely distinguish illegal from legal harvest, and site-level poaching studies do not scale to global conservation planning. Here we develop a global predictive model of poaching probability for terrestrial mammals, integrating 1,168 georeferenced poaching occurrences with ecological and anthropogenic drivers. Hunted mammal richness and accessibility to cities were the strongest predictors, while economic effects varied with income group. Poaching probability peaked across Southeast Asia, sub-Saharan Africa, and parts of the Americas and Europe, with species richness dominant across most regions and accessibility dominant in remote areas. This work provides a scalable tool for prioritising enforcement, protected-area investment, and demand-reduction policy under the Global Biodiversity Framework.

Main Text

Wild terrestrial mammals are facing a global extinction crisis, with a significant decline in both population size and geographical ranges[1,2]. This decline is driven by a suite of anthropogenic pressures[3] that, acting synergistically, amplify the threats beyond what each pressure would pose individually. Among these, hunting is the leading threat to terrestrial mammals, depleting populations and eroding mammal richness globally[1,4]. As species ranges contract and populations become increasingly confined to smaller and more fragmented areas, they become disproportionately exposed to hunting[5], as it is most intense along forest edges[5,6], roads and human settlements[7,8], and range contraction itself concentrates individuals into smaller areas, increasing encounter rates and potentially facilitating harvest.

Although hunting has been a cornerstone of human livelihoods throughout history[9], its sustainability depends on whether harvest rates remain within the demographic capacity of target populations to recover[10]. When practiced sustainably, hunting can coexist with healthy wildlife

populations and provide a legitimate, culturally important, and often irreplaceable source of nutrition, income, and identity for indigenous people and rural communities[11,12,13]. In many tropical regions, wild meat continues to provide an essential source of food security and livelihoods, whereas in developed countries hunting is more commonly practiced for recreational, cultural, or management purposes rather than as a primary source of subsistence[14]. Yet, as human populations and anthropogenic footprints expand, wildlife demand is expected to rise, pushing harvest rates beyond what many wild populations can sustain[15]. Illegal hunting (hereafter poaching) accelerates this dynamic further: unconstrained by quotas, seasonal restrictions, and wild population monitoring that govern legal harvest, it can go beyond the bounds of sustainable offtake, driving population declines and undermining the very resource base subsistence communities depend on[16,17]. In higher income countries, where subsistence need is rarely the motivation, poaching instead threatens to reverse conservation gains achieved through decades of wildlife protection and recovery efforts[18].

Poaching exerts severe and well-documented impacts on terrestrial mammal populations[19], particularly in the tropics, driving local extinctions, suppressing population growth rates, and restructuring community composition toward smaller-bodied, less commercially valuable species[20,21,22]. These impacts fall disproportionately on large-bodied species, which yield the greatest returns per unit of hunting effort[21] and possess commercially valuable anatomical parts that command high prices in illegal markets[1,23]. These species are characterized by slow reproductive rates and low population growth, making them the least able to sustain elevated harvest and the most vulnerable to extinction under continued illegal hunting[24]. Beyond direct population loss, the removal of large-bodied species triggers cascading effects across ecological communities[25,26,27], given their role as seed dispersers, apex predators and ecosystem engineers[28]. Yet, despite its recognised importance as a threat, spatial dynamics of poaching remain poorly understood relative to other drivers of biodiversity loss[20].

Threat mapping has become an essential tool for prioritising conservation investments, guiding protected area placement, and allocating enforcement resources under frameworks such as Kunming-Montreal Global Biodiversity Framework (KMGBF)[29]. Yet, generalised human-pressure indices, such as Human Footprint Index[30,31] or multi-threat mapping frameworks, do not disaggregate hunting as a distinct threat and so cannot capture the dynamics specific to poaching.

Unlike habitat loss, which can be monitored through remote sensing, poaching is cryptic, spatially heterogeneous and driven by a shifting combination of ecological opportunity, market access, and socioeconomic conditions that vary substantially across regions[32]. For example, proximity to roads and urban centres determines how easily hunters can access wildlife and transport products to market[33], while local economic conditions shape the motivation to engage in illegal harvest in the first place[34,35]. Understanding where these conditions converge is therefore essential for predicting where poaching is most likely to occur. Recent studies have made significant progress mapping hunting-related threats to wildlife at broad scale, substantially improving our understanding of where and why hunting poses substantial risk to vertebrate populations[8,36,37]. However, these approaches generally treat hunting as a single threat category, spanning legal and illegal harvest[36,8,38], or infer risk from species-level assessments, such as IUCN Red List threat classifications [37,39]. Nevertheless, illegal hunting cannot be effectively addressed through the same instruments used to regulate legal harvest, nor by assuming species might be hunted uniformly across their range. Because data on illegal activity are difficult to obtain, spatially explicit assessments of poaching probability have instead remained largely confined to small, intensively monitored sites, primarily protected areas, where ranger patrol data yield localised incident records[40,41]. While informative, these site-level studies are difficult to extrapolate to broader landscapes, particularly where monitoring capacity is limited. Consequently, no global map of poaching probability exists across the terrestrial surface, limiting both the targeting of conservation action and the assessment of progress towards the KMGBF targets (e.g. Target 5: Ensure Sustainable, Safe and Legal Harvesting and Trade of Wild Species). Such a tool could support the spatial allocation of targeted responses, from law enforcement investment and anti-poaching patrols to awareness campaigns and alternative livelihood programmes.

Here we address this gap by developing a global, spatially explicit model of poaching occurrence probability for terrestrial mammals. Recent public releases of large-scale poaching incident data now provide georeferenced records at a scale that allows poaching events to be modelled well beyond individual sites. Using 1,168 georeferenced poaching occurrences and a suite of environmental and anthropogenic predictors, we use Generalized Additive Models (GAMs) and Random Forests (RF) to model the relationships between poaching occurrences and anthropogenic and ecological drivers. Our predictors capture market accessibility, infrastructure, and ecological opportunity, including travel time to cities, road proximity, night-time light intensity, gross domestic

product (hereafter GDP), hunted mammal richness, and distance to strict protected areas (see Extended Data Table 1 for the expected relationship between each predictor and poaching probability). For two key predictors, we explicitly account for geographic and socioeconomic context: GDP effects are modelled conditional on country income group, and hunted mammal richness effects are modelled conditional on biogeographic realm, reflecting the expectation that these relationships are not globally uniform. The full analytical workflow is presented in Fig. 1.

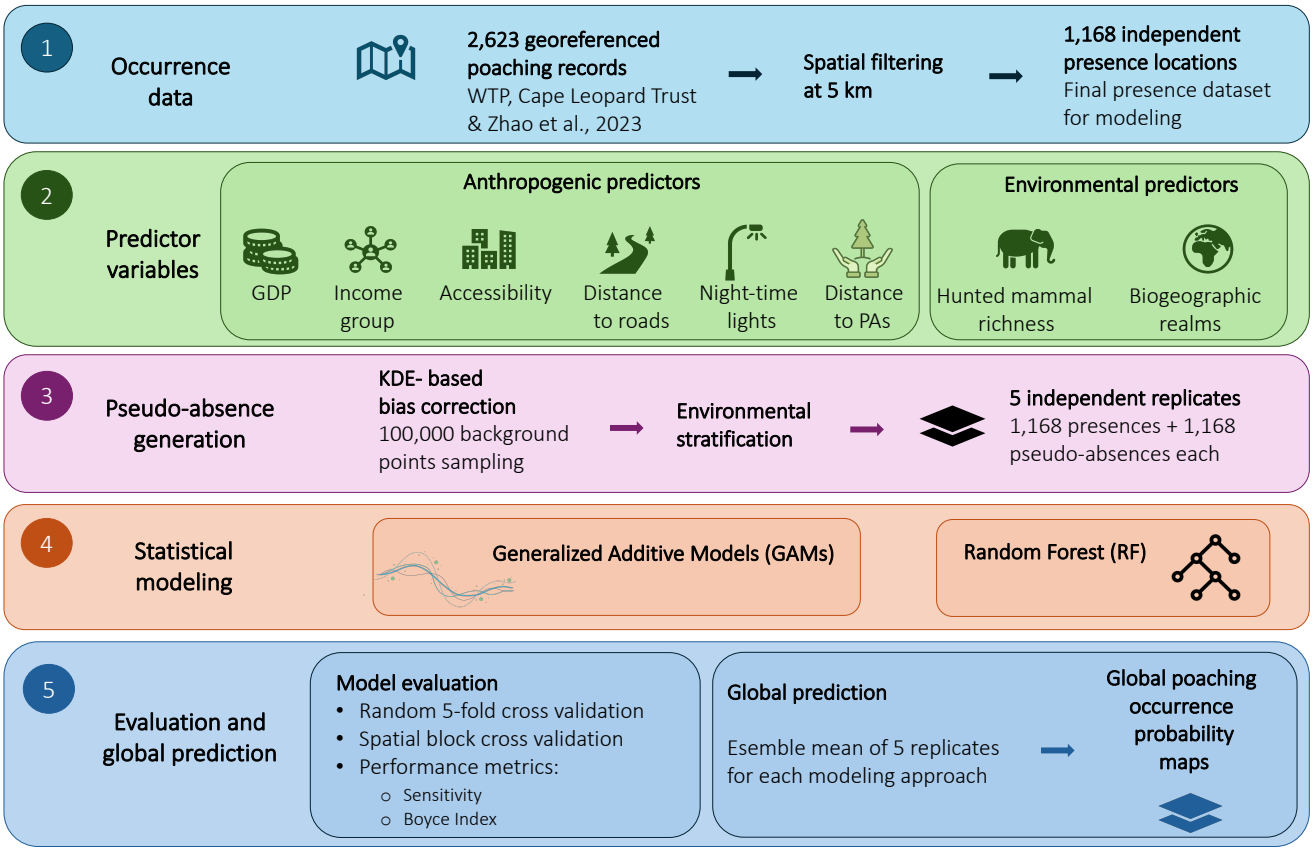


Figure 1. Analytical workflow for the global poaching occurrence probability maps. **1**: Georeferenced poaching occurrences were compiled from three sources and thinned at 5 km. **2**: Nine candidate predictors (see Extended Data Table 1 for the rationales) were selected and assessed for collinearity. **3**: Pseudo-absences for poaching records were generated using a KDE-based bias correction procedure across five independent replicates. **4**: Poaching occurrence probability was modelled using Generalized Additive Models and Random Forests. **5**: Models were evaluated using random and spatial block cross-validation and applied to generate global ensemble prediction maps.

Results

Global distribution of poaching records

Following data cleaning, the combined dataset comprised 2,623 poaching records involving 177 terrestrial mammal species belonging to nine mammalian orders, distributed across 80 countries and five continents (Supplementary Fig. S1). All records were aggregated to a 5 × 5 km grid and a single occurrence retained per cell regardless of source (see Methods), yielding 1,168 independent poaching occurrences used for subsequent analyses (Fig. 2a). Poaching occurrences were strongly clustered geographically, with most concentrated in Asia (n = 632) and Africa (n = 396), and the dataset exhibited marked taxonomic bias toward a limited number of mammal families, with Rhinocerotidae, Felidae, and Elephantidae together accounting for over 70% of records for which family identity was reported (Fig. 2b–c).

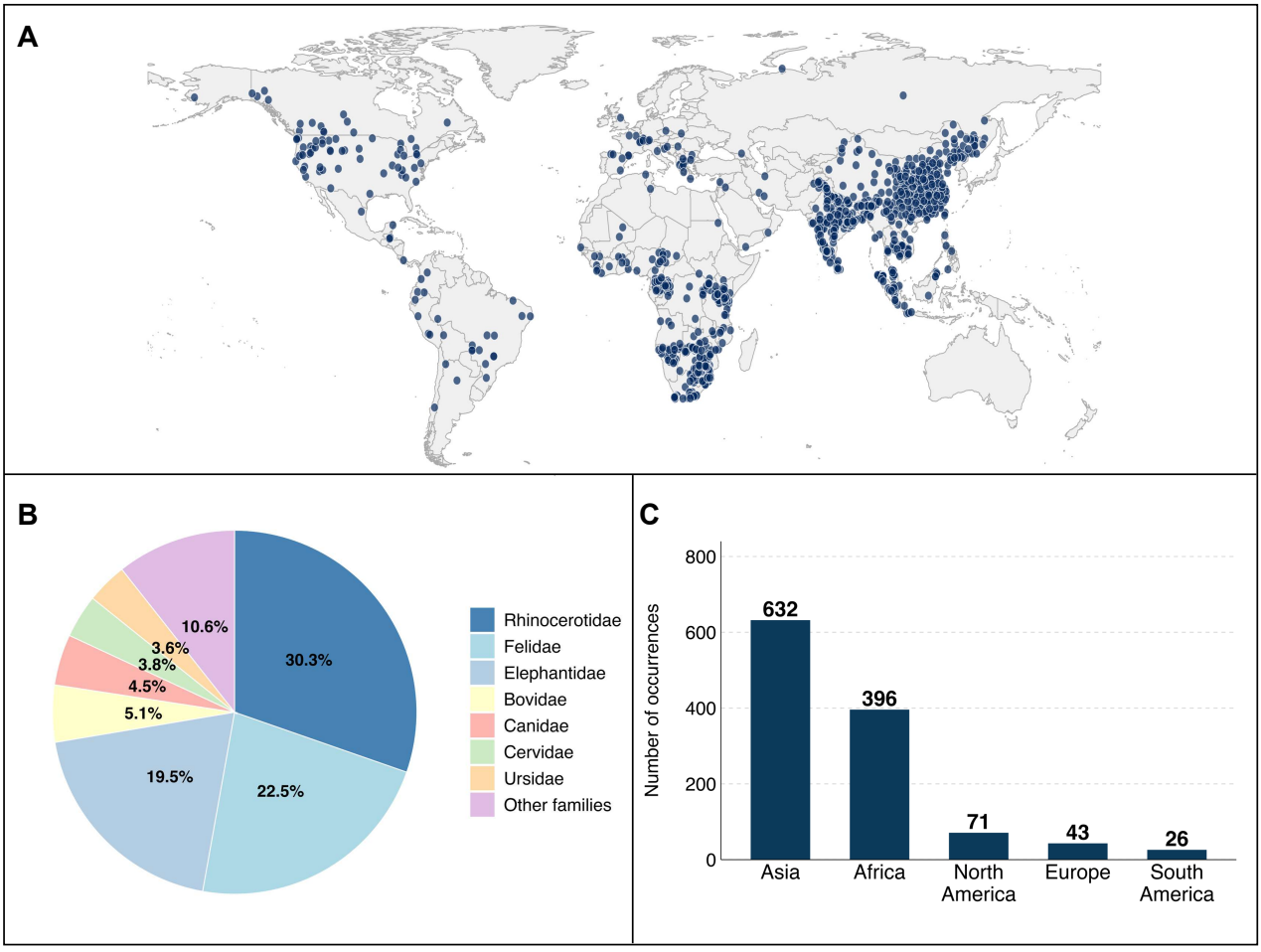


Figure 2. Global distribution and taxonomic composition of poaching records used in the analysis. **a,** Spatial distribution of 1,168 georeferenced poaching occurrences retained after spatial filtering at 5

km resolution. **b,** Relative contribution of the most frequently represented mammalian families in the dataset. Families contributing less than 3.6% of records were grouped as "Other families". **c,** Number of poaching sites by continent.

Ecological and anthropogenic drivers of poaching occurrence probability

Prior to model fitting, human population density was found to be strongly correlated with travel time to the nearest city and was excluded from final analyses based on collinearity (Pearson r = -0.77; Supplementary Fig. S2); travel time to the nearest city was retained because it provides a more direct proxy for accessibility to urban markets, which is known to be a primary driver of illegal harvest. Hunted mammal richness was the strongest predictor in both modelling frameworks (Fig. 3a). In the GAM, where richness effects were fitted separately for each realm, the effect was strongest in the Afrotropical realm (Chi-square = 126.0 ± 9.7; Fig. 3b), whereas in RF, which estimates a single effect across realms, mean permutation importance was 0.069 ± 0.010. Hunted richness showed a positive relationship with predicted probability across all focal biogeographic realms, though the strength and shape of this relationship varied substantially (Fig. 3c). The relationship was most pronounced in the Afrotropical realm, where richness ranged from 1 to 58 hunted species per grid cell (mean = 30.4), and poaching probability increased steeply across the full richness gradient. A similarly strong increase was observed in the Palearctic realm (Chi-square = 75.6 ± 9.2; richness range: 0–35). In the Indomalayan realm (Chi-square = 53.8 ± 9.9; richness range: 0–50), poaching probability rose rapidly at low richness levels before plateauing at approximately 20–30 species per cell. The richness-poaching relationship was negligible in the remaining realms (Chi-square < 6 for all), partly reflecting sparse training data in the Australasian (n = 2 occurrences) and Oceanic (n = 1) realms. The corresponding RF response curve for hunted mammal richness was comparatively flat at a high poaching probability value (Fig. 3d).

Accessibility to cities was the second strongest independent predictor in GAMs (Chi-square = 43.2 ± 7.3) and in RFs permutation importance (0.050 ± 0.007). In both modelling approaches, predicted poaching occurrence probability declined with increasing travel time to the nearest city (Fig. 3e,f), indicating that poaching probability was concentrated in areas with greater accessibility to urban centres. In GAMs, GDP interaction with income was the third strongest interaction term overall, driven primarily by the low-income group (Fig. 3a,b), and the shape of the relationship varied across income groups (Fig. 3g). In low-income countries (Chi-square = 31.0 ± 13.8; median log GDP = 3.21, ~$1,600/capita), poaching probability increased monotonically with GDP, suggesting that, within

those countries, even modest economic activity amplifies wildlife exposure to illegal harvest by improving market access without yet generating alternative livelihoods. In upper-middle income countries (Chi-square = 26.0 ± 14.7; median log GDP = 4.04, ~$9,600/capita), the relationship was unimodal, peaking at intermediate GDP values (logGDP = 3.79, ~$6,200/capita) before declining. GDP effects were substantially weaker in high income OECD (Organisation for Economic Co-operation and Development membership; Chi-square = 2.7 ± 2.6), high income non-OECD (1.4 ± 1.0), and lower-middle income contexts (2.7 ± 2.6). In RF models, the response curve for GDP (Fig. 3h) showed a unimodal pattern, dipping slightly at the lowest GDP values before rising sharply to a peak at intermediate GDP and then declining toward a plateau at higher values; a shape that partly mirrors the GAM's upper-middle-income curve (Fig. 3g). Night-time light intensity (GAM Chi-square = 15.4 ± 8.3; RF permutation importance = 0.036 ± 0.004), distance to roads (GAM: 4.7 ± 1.5; RF: 0.035 ± 0.006), and distance to strict protected areas (GAM: 3.1 ± 2.7; RF: 0.020 ± 0.002) were the weakest predictors across both approaches. Response curves for these three predictors are presented in Supplementary Fig. S3.

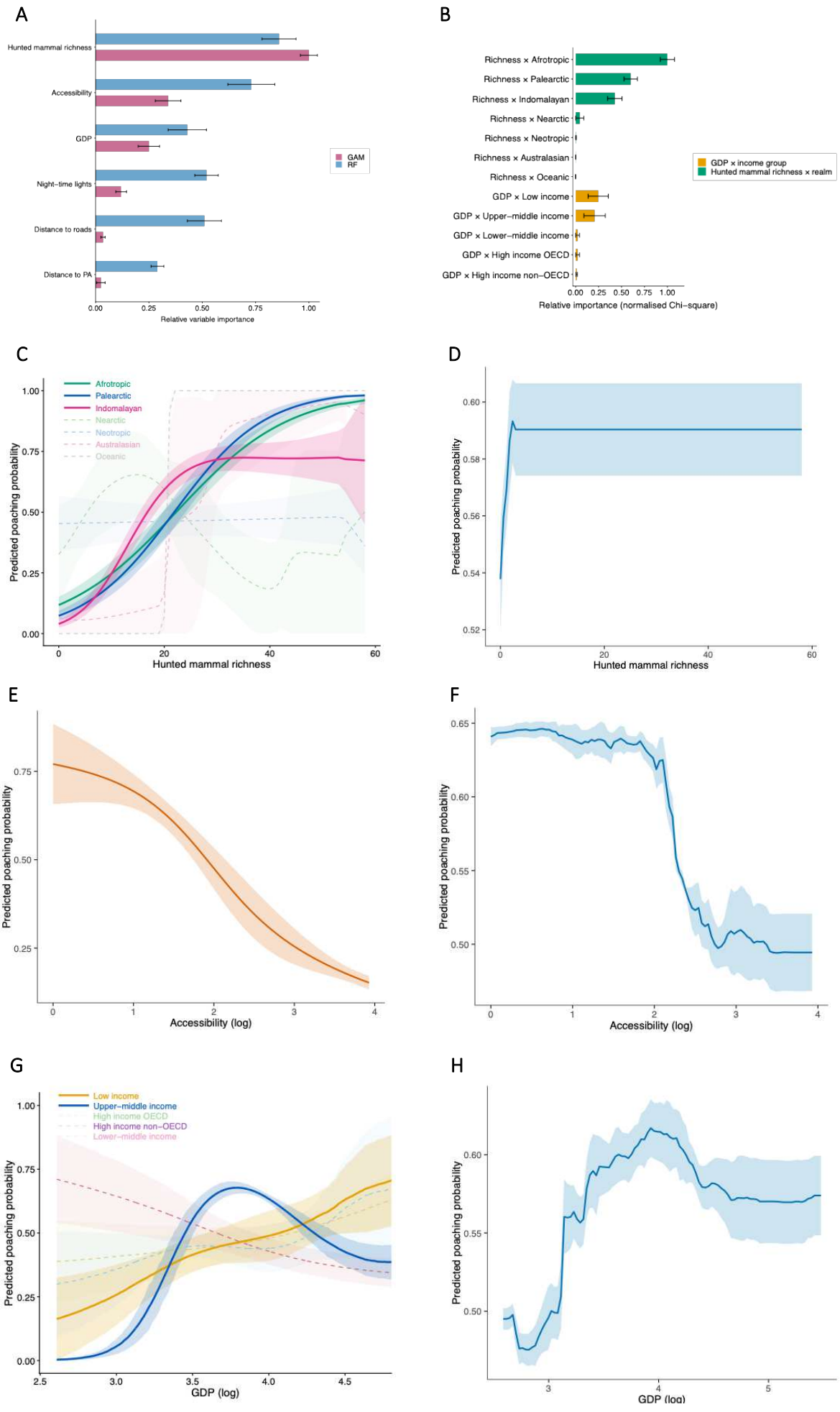

A
Hunted mammal richness
Accessibility
GDP
Night−time lights
Distance to roads
Distance to PA
GAM
RF
0.00
0.25
0.50
0.75
1.00
Relative variable importance
B
Richness × Afrotropic
Richness × Palearctic
Richness × Indomalayan
Richness × Nearctic
Richness × Neotropic
Richness × Australasian
Richness × Oceanic
GDP × Low income
GDP × Upper−middle income
GDP × Lower−middle income
GDP × High income OECD
GDP × High income non−OECD
GDP × income group
Hunted mammal richness × realm
0.00 0.25 0.50 0.75 1.00
Relative importance (normalised Chi−square)
C
Afrotropic
Palearctic
Indomalayan
Nearctic
Neotropic
Australasian
Oceanic
Predicted poaching probability
0.00 0.25 0.50 0.75 1.00
0 20 40 60
Hunted mammal richness
D
Predicted poaching probability
0.52 0.54 0.56 0.58 0.60
0 20 40 60
Hunted mammal richness
E
Predicted poaching probability
0.25 0.50 0.75
0 1 2 3 4
Accessibility (log)
F
Predicted poaching probability
0.50 0.55 0.60 0.65
0 1 2 3 4
Accessibility (log)
G
Low income
Upper−middle income
High income OECD
High income non−OECD
Lower−middle income
Predicted poaching probability
0.00 0.25 0.50 0.75 1.00
2.5 3.0 3.5 4.0 4.5
GDP (log)
H
Predicted poaching probability
0.50 0.55 0.60
3 4 5
GDP (log)

Figure 3. Relative importance and response curves of poaching risk predictors. **a,** Relative variable importance for GAM (normalised Chi-square) and RF (permutation importance), each scaled 0–1. **b,** Relative importance of the two GAM interaction terms tested (hunted mammal richness × realm; GDP × income group), shown separately for each realm/income level (normalised Chi-square). **c,** GAM-predicted effects of hunted mammal richness across biogeographic realms; solid lines indicate realms with the strongest interaction effects (Afrotropical, Palearctic, Indomalayan), dashed lines indicate realms with negligible interaction effects (Nearctic, Neotropic, Australasian, Oceanic). **d,** Pooled RF partial dependence for hunted mammal richness. **e,** GAM-predicted effect of accessibility to cities (log scaled). **f,** Pooled RF partial dependence for accessibility (log). **g,** GAM-predicted effects of GDP (log) across income groups; solid lines indicate income groups with the strongest interaction effects (low income, upper-middle income), dashed lines indicate income groups with negligible interaction effects (lower-middle income, high income OECD, high income non-OECD); income groups follow World Bank classifications, with OECD/non-OECD distinguishing high-income countries by Organisation for Economic Co-operation and Development membership. **h,** Pooled RF partial dependence for GDP (log). Solid lines in from c to h represent mean predictions across five pseudo-absence replicates; shaded areas indicate ±1 SD across replicates.

Spatial variation in predictor dominance

To characterize how the relative influence of each predictor varies geographically, we identified, for each grid cell, which predictor contributed most strongly to the GAM predicted probability of poaching (Fig. 4). Hunted mammal richness was the locally dominant predictor across the overwhelming majority of the terrestrial surface, including most of Eurasia, Africa and South America, matching its status as the single strongest predictor overall (Fig. 3a). Accessibility to cities was instead locally dominant primarily in remote, low-rich regions, including northern Canada and central Australia, whereas GDP in more scattered areas, concentrated in South America and parts of southern Africa. Road density and night light intensity were locally dominant in a few grid cells, respectively in some parts of southeast Asia and South America. Distance to protected areas was never a locally dominant predictor in any grid cell.

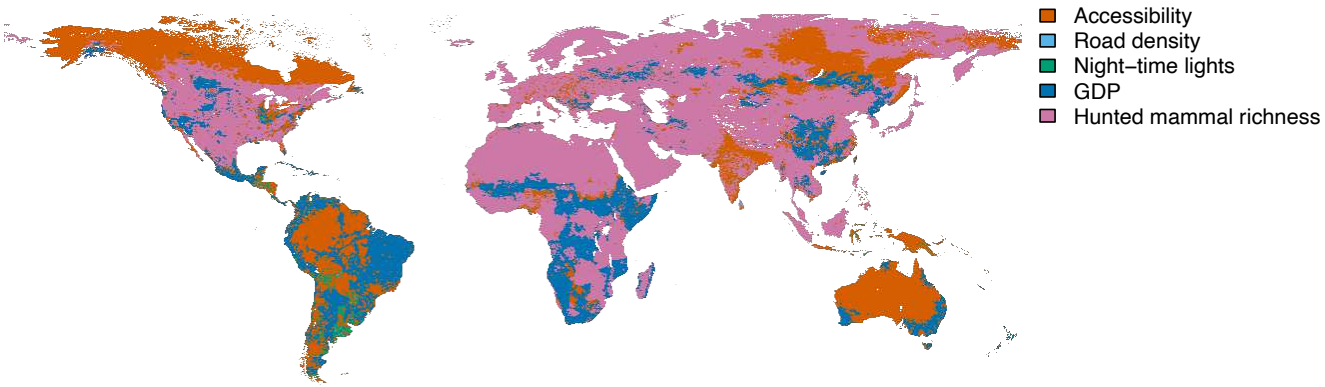


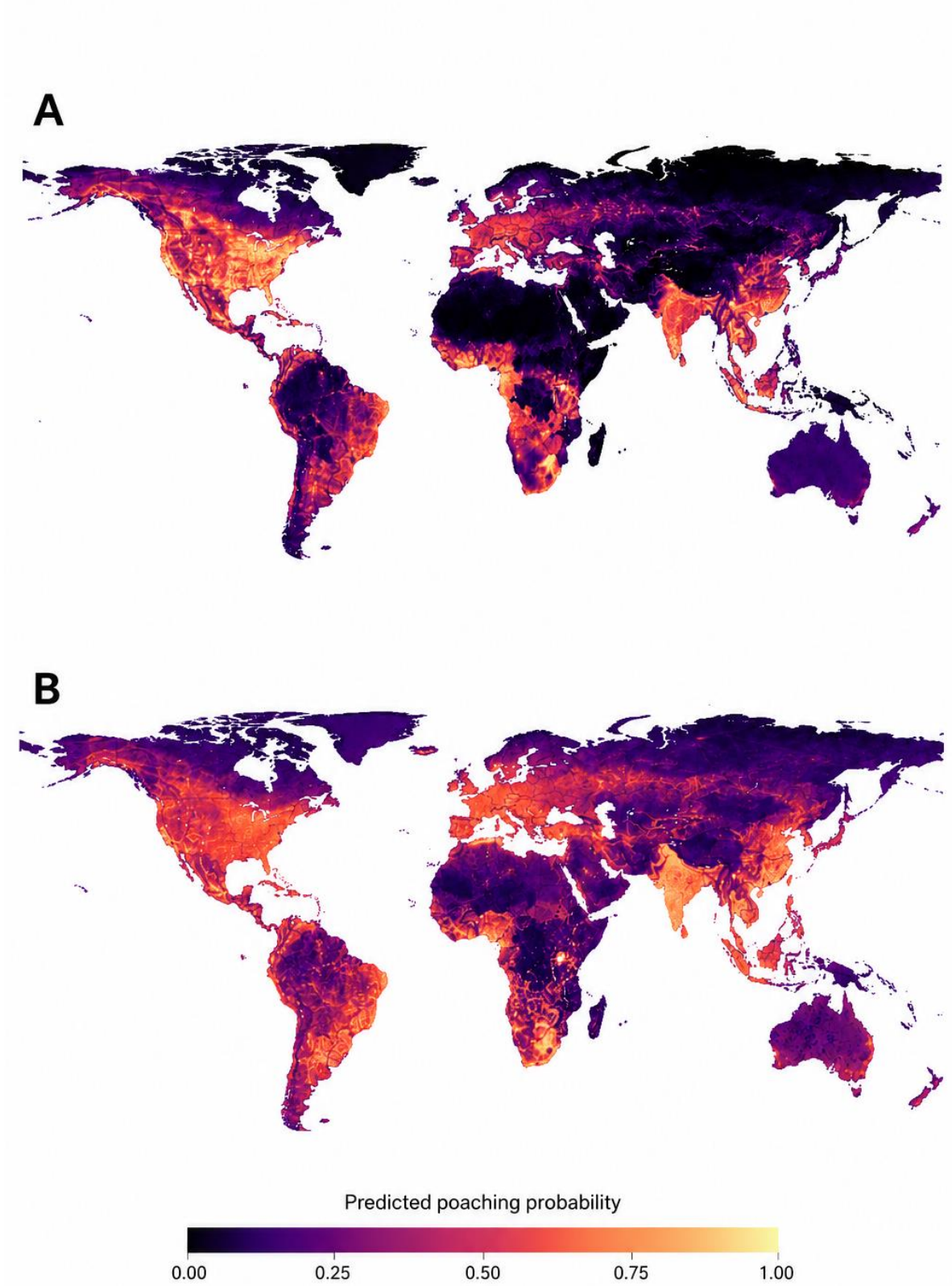
Figure 4. Spatial variation in the locally dominant predictor of poaching risk. For each grid cell, the predictor contributing most strongly to the GAM-predicted probability of poaching is shown. Distance to protected areas is omitted from the legend, as it was never the locally dominant predictor in any grid cell.

Global patterns of predicted poaching risk

Under spatial block cross-validation, GAM achieved a mean sensitivity of 0.791 ± 0.005 and Boyce index of 0.956 ± 0.009 (mean ± s.d. across the five pseudo-absence replicates), while RF achieved a mean sensitivity of 0.806 ± 0.005 and Boyce index of 0.967 ± 0.003. Both models predicted strong spatial heterogeneity in global poaching risk, with broadly consistent geographic patterns despite differences in modelling approach (Fig. 5a,b). In both models, areas of highest predicted probability were concentrated in South and Southeast Asia -particularly the Indian subcontinent, Indochina, southern China, and the Indonesian archipelago-, sub-Saharan Africa, parts of Europe, and substantial portions of the Americas, including eastern North America and Amazon margins of South America. Remote, sparsely populated, and climatically extreme regions -including the Sahara, Arabian Peninsula, central Australia, and boreal and Arctic zones- consistently showed low predicted risk across both models. Predicted geographic patterns were highly concordant between the two models, though they differed in the sharpness of the transition between high- and low-risk areas, a distinction also evident in the global distribution of predicted values (Supplementary Fig.S4). The distribution of GAM predicted poaching probability was widely spread and right-skewed (0.31 ± 0.25, skewness = 0.69), spanning nearly the full range of possible values and identifying both

extensive low-risk areas (23.7% of the terrestrial surface predicted <0.1) and a smaller but non-trivial hotspot fraction (1.1% predicted >0.9). RF predictions were instead tightly compressed around a higher central value (0.48 ± 0.14, skewness = 0.49), with 98.6% of the land surface falling within the intermediate 0.2-0.8 range, no grid cell was predicted below 0.1, and only four cells (<0.01% of land area) exceeded 0.9. Because GAM retains this discriminatory capacity across the full risk gradient while RF does not, we treat GAM as the primary interpretive surface throughout the remainder of this study; RF is retained as an independent, non-parametric robustness check (see Methods). Using the maximum sum of sensitivity and specificity[42] (maxSSS) threshold derived for each model (GAM = 0.454; RF = 0.480), GAM classified 31.8% of the terrestrial surface as at risk of poaching, compared with 48.9% under RF.

To assess the reliability of spatial extrapolation, we computed the Multivariate Environmental Similarity Surface (MESS) across the prediction domain (Supplementary Fig. S5). Most of the terrestrial surface (97.1%) fell within the range of environmental conditions represented in the training data, with a further 0.3% at the exact boundary of the training data. True extrapolation (MESS < 0) was confined to 2.7% of the terrestrial surface, concentrated along the high-Arctic margins of northern Canada and Greenland.



245

246 **Figure 5.** Global predictions of poaching probability derived from GAMs (**a**) and RF (**b**). Maps show
247 the mean predicted probability of poaching occurrence across five pseudo-absence replicates for
248 each modelling approach. Warmer colours indicate higher predicted risk.

Regional patterns of poaching probability

Predicted poaching probability varied substantially across continents, biogeographic realms, and countries. At the continental scale, South America showed the highest median predicted probability (0.47, interquartile range 0.36–0.59), closely followed by North America (0.46, 0.32–0.64), while Europe and Asia showed the lowest, both with a median of 0.26 (interquartile ranges 0.19–0.40 and 0.20–0.45, respectively; Fig. 6a). At the biogeographic realm scale, the Indomalayan realm showed the highest median predicted probability (0.69, 0.56–0.78), while the Oceanic realm showed the lowest and most homogeneous predictions (0.24, 0.20–0.25; Fig. 6b). Within each continent, predicted probability varied substantially among countries, with full rankings provided in Fig. 6c.

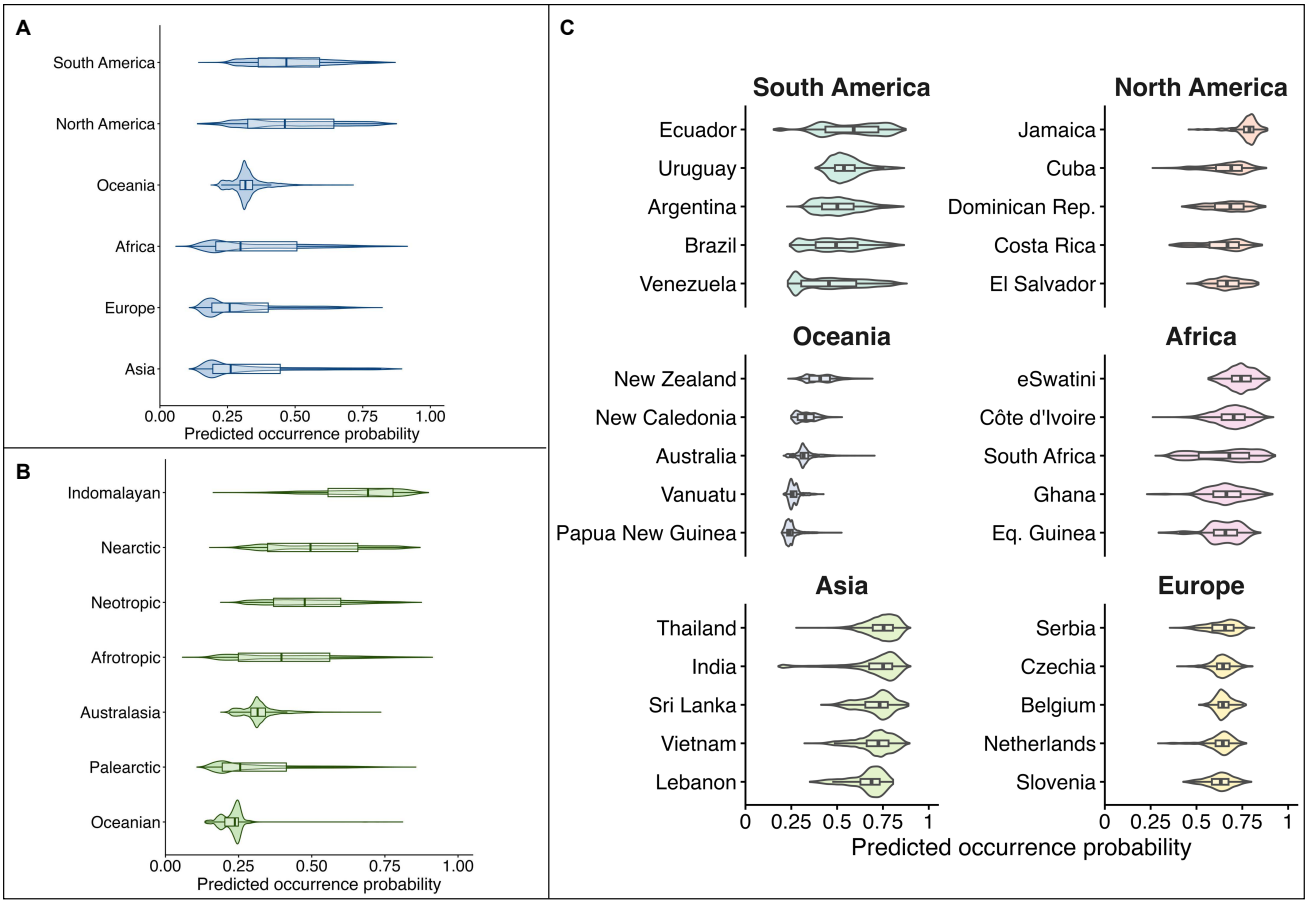


Figure 6. Regional patterns of predicted poaching probability. Each panel shows the distribution of cell-level predicted values, with the central boxplot indicating the median and interquartile range: **a,** distribution by continent. **b,** distribution by biogeographic realm. **c,** distribution for the five countries with the highest median predicted probability within each continent. Countries with a total land area below 10,000 km² were excluded from country-level summaries as the 5 km spatial

resolution of the model is insufficient to provide reliable national-scale estimates for territories of this size.

Discussion

Existing threat assessments focused on hunting have generally pooled legal and illegal harvest into a single, undifferentiated category[36,37], without resolving where illegal offtake itself concentrates. This study addressed this gap by targeting poaching occurrence specifically, at global extent. Poaching risk consistently tracked the intersection of species availability, human accessibility and economic incentive, with different factors dominating in different regions of the world. This pattern was not confined to the tropical systems where poaching's ecological toll is best documented, and predicted risk aligns closely with existing defaunation and hunting-pressure maps, most notably across South and Southeast Asia, sub-Saharan Africa, and the Amazon periphery[43]. This concordance suggests that the conditions structuring poaching risk are general enough to be inferred from ecological and socioeconomic data alone, making it possible to extend risk assessments beyond the handful of regions where poaching has historically been studied most intensively.

Hunted mammal richness was, by far, the most important predictor of poaching probability in both modelling approaches, in line with richness's role as the locally dominant predictor across nearly the entire terrestrial surface. This relationship likely arises not from richness per se but because greater target-species diversity expands the range of commercially valuable species available to hunters and sustains broader wildlife trade networks. GAMs showed this relationship is not spatially uniform and its effect was proportionally stronger in the Afrotropical, Palearctic, and Indomalayan realms than elsewhere. A plausible explanation is that poaching in these realms is disproportionately structured by trade-driven networks that actively target areas of high species diversity and commercial value[44], whereas in other realms offtake is less concentrated by richness and more evenly distributed across the landscape, though it cannot be tested directly yet with our occurrence data. For instance, the Australasian and Oceanic realms could not be reliably assessed given their small sample size and therefore these realm-specific estimates should be interpreted with corresponding caution.

Human accessibility was the second most important predictor, with poaching probability decreasing as travel time to the nearest urban centre increased. This finding aligns with a broad literature linking transport infrastructure to illegal harvest by reducing the time, effort and logistical cost of reaching wildlife and moving products to markets[36,8]. Road proximity reinforces this pattern as poaching probability also decreased with increasing distance from roads, consistent with other studies[40], reflecting the role of road networks in extending the spatial reach of hunters into otherwise inaccessible landscapes. Together, these two predictors point to a coherent mechanism: poaching concentrates where the friction of accessing wildlife and urban markets is lowest, making human accessibility the primary spatial organiser of poaching pressure at landscape scale. This has important implications for the future as the expansion of road networks is accelerating, and these changes are mostly expected in Africa, South and East Asia, and South America[45], regions where predicted poaching probability already exceeds our classification threshold across substantial areas. As remoteness declines, wildlife populations currently buffered by isolation are likely to become increasingly exposed, compressing the geographic refugia available to wildlife in the only inaccessible landscapes that will be left[36].

Economic conditions were also an important predictor, with the strength and shape of the relationship varying substantially across income groups. In low-income contexts, poaching probability rose with GDP, indicating that even modest economic growth amplifies illegal harvest pressure, likely by improving market access and the logistical capacity to move wildlife products, without yet generating the alternative livelihood opportunities that might reduce dependence on illegal harvest. In upper-middle income contexts, the relationship was unimodal, consistent with a transitional dynamic in which initial economic development increases commercial demand while continued growth eventually provides economic alternatives to illegal harvest[46]. This pattern likely reflects the nature of our datasets, which is dominated by carcasses of large species targeted for specific body parts, a signature of commercially driven poaching rather than subsistence offtake, whose evidence is rarely detectable in the field. The GDP results should therefore be read as characterising the geography of trade-driven poaching specifically, not as evidence that poaching is absent in low GDP areas. More broadly, these results converge with arguments in the literature that poverty *per se* is not the primary driver of illegal hunting in low-income regions, and that economic inequality (the gap between what legitimate economic structure can provide and what communities need) may better explain engagement in illegal harvest[34]. However, our model cannot

test this distinction directly, as it captures broad GDP levels, and this should be read as a hypothesis our results suggest.

Spatially, the Indomalayan realm emerged as the most pronounced hotspot, driven by the simultaneous convergence of high hunted mammal richness, dense road networks and strong market connectivity, with richness as the locally dominant driver throughout. India stands out within the realm, where exceptional species richness and high human accessibility interact to produce high and spatially extensive predicted probability, a pattern echoing documented illegal harvest pressure on the subcontinent[47]. China's populous eastern regions similarly showed elevated predicted probability, reflecting elevated hunted mammal richness, accessibility and GDP, while the less accessible western regions show low predicted probability[48]. In sub-Saharan Africa, predicted probability was concentrated along the west coast, in the corridor spanning South Africa and Zimbabwe, and the East African region encompassing Uganda, Kenya, and Tanzania, supporting existing knowledge of poaching pressure on the continent[7]. Richness remains the dominant driver across most of the continent, except in the South Africa-Zimbabwe corridor and in the area immediately south of the Sahel region, where GDP instead governs local risk. In South America, the highest predicted poaching risk extended across the Andean nations and along the eastern coasts of Brazil, Uruguay, and Argentina, while the core area of the Amazon basin currently shows comparatively low predicted risk, primarily reflecting the inaccessibility of its most remote areas, currently the region's dominant buffering factor, rather than an absence of hunting motivations. However, the Amazon faces accelerating threats from deforestation, illegal hunting[49], and expanding road networks, and proposals such as Brazil's BR-319 highway continue to advance[50]. Our results suggest that new road construction would lower barriers to illegal harvest in one of the world's most biodiverse and genetically distinct mammal communities. Finally, a large area of elevated predicted poaching probability in parts of North America and Europe reflects high accessibility and moderate hunted mammal richness, conditions strongly associated with poaching elsewhere, and illegal hunting does occur in the region, driven by entirely different motivations, at levels that are likely substantially underreported[14,51,52]. The gap between predicted environmental suitability and realised poaching pressure in these regions might point to the suppressive effect of strong regulatory frameworks and enforcement capacity, as well as the underlying socioeconomic conditions that determine whether poaching becomes a viable option for communities in the first place[53]. This suppression is itself conditional on governance and finer-scale economic factors, such

as local income inequality, not captured by the country-level GDP and income classifications included in our model, which should be treated as a source of predictive uncertainty in these regions.

The global map of poaching probability presented here offers a practical foundation for conservation prioritisation under the Kunming-Montreal Global Biodiversity Framework's targets[29]. Current PA expansion efforts are largely guided by biodiversity value[54] but rarely incorporate systematic information on where illegal hunting is most likely to occur. Areas of high predicted poaching occurrence currently outside formal protection represent priority candidates for new designation, while areas already under protection that coincide with high predicted occurrence warrant targeted investment in boundary management and enforcement. The context-dependence of key drivers also suggests that a single, uniform conservation strategy is unlikely to be equally effective everywhere. Where accessibility dominates predicted risk, interventions that raise the practical cost of reaching wildlife may be most relevant, while where richness or economic drivers dominate, different levers are likely to matter more. Translating this spatial heterogeneity into specific policy instruments would, however, require evaluation beyond the scope of the present study.

We note that our dataset reflects where illegal hunting is detected and reported more than where it occurs. Detection probability is unevenly distributed globally, with regions lacking monitoring infrastructure almost certainly underrepresented, and poachers may strategically avoid areas of known enforcement activity, further decoupling occurrence from detection. The model therefore captures environmental suitability for poaching occurrence rather than realised harvest intensity. Governance capacity and corruption are likely important modulators of this gap[55], suppressing realised occurrences where institutions are strong and amplifying it where they are not, but the absence of high-resolution, globally consistent data on these factors precluded their inclusion as explicit predictors. The dataset is also dominated by evidence of commercially driven poaching, and illegal hunting for subsistence contexts (e.g. through wire snares) is underrepresented. A more complete picture would require integration of community-based monitoring data and ranger patrol records from a broader range of governance contexts. Finally, the analysis represents a static snapshot: the global risk landscape will shift as infrastructure expands, economies develop, and

wildlife populations change. Hence, dynamic, regularly updated assessments represent an important direction for future work.

By establishing the first global baseline of poaching occurrence for terrestrial mammals, this study opens a new line of spatially explicit research into one of the most pervasive yet poorly mapped threats to wildlife. As poaching occurrence datasets grow, predictor layers improve, and monitoring expands beyond protected area boundaries, the framework developed here can be refined, validated, and ultimately updated to track how the spatial patterns of illegal hunting shift under future scenarios. More immediately, the predicted maps offer a starting point for evidence-based conservation prioritisation, directing attention and resources toward the regions and conditions where the pressure on wildlife is greatest, and where the opportunity to intervene before irreversible decline remains open.

Methods

Poaching occurrence data

Spatially referenced records of poaching events on terrestrial mammals at a global scale were obtained from the Wildlife Trade Portal (WTP)[56], an interactive platform that aggregates records of wildlife trade and poaching events from publicly available media reports, NGO publications, and enforcement records. We extracted all the records that explicitly reported poaching-related mortality, defined as locations where dead animals were documented with clear evidence attributing the killing to illegal hunting (i.e., carcasses showing signs of intentional removal of commercially valuable body parts such as horns, ivory or pelts). Each record was treated as a poaching event and georeferenced using the longitude and latitude provided by the WTP. We only kept spatial data on origin locations of poaching occurrences. To improve geographic and taxonomic coverage, we supplemented these records with two additional datasets. First, we incorporated 641 snare presence locations, treated as direct evidence of illegal hunting as snares are prohibited in South Africa, and six confirmed carcasses, both detected during intensive snare patrol conducted from June 2019 to June 2020 in Boland Mountain region of the Western Cape, South Africa, provided by the Cape Leopard Trust[57]. Second, we added 242 poaching occurrence records collected between 2014 and 2020 from a dataset published by Zhao et al., 2023[58] of mammal poaching in China, increasing representation from a region otherwise underrepresented in the WTP (Supplementary Fig. S1a). To reduce spatial clustering and sampling bias, all poaching

occurrences were aggregated to a 5x5 km grid, and a single presence record was retained per cell regardless of source. This yielded 1,168 unique presence locations used for subsequent analyses. Although occurrence records spanned the full study period, the large majority were concentrated after 2014 (Supplementary Fig. S1b), that could reflect both genuine increases in poaching pressure or, more likely, improvements in documentation and data aggregation over time[59]. The geographic distribution of records was also uneven, reflecting spatial variation in both poaching activity and reporting effort across regions. This spatial heterogeneity in detection effort was explicitly accounted for in the pseudo-absence selection procedure, as described below.

Modelling framework

The objective of this study was to identify broad-scale spatial correlates of poaching occurrence rather than temporal variation in poaching dynamics. Consequently, all environmental predictors were represented as temporally static surfaces describing long-term average conditions across the study period. For variables available as annual time series, yearly rasters were averaged to produce a single layer representative of prevailing anthropogenic or ecological conditions. To ensure temporal consistency between poaching records and the predictor layers, which reflect conditions from approximately 2010 onward, poaching records reported prior to 2010 from WTP were excluded, restricting the final dataset to records spanning 2010–2025. Models therefore estimate the spatial probability of poaching occurrence as a function of persistent environmental gradients rather than interannual variability in environmental and anthropogenic conditions. The study extent covered the global terrestrial surface, excluding Antarctica, at a spatial resolution of 5 × 5 km.

Predictors

We selected nine candidate predictors representing hypothesised anthropogenic and ecological drivers of poaching occurrences (Extended Data Table 1): accessibility, measured as travel time to the nearest city[60]; distance to roads[45]; night-time light intensity[61]; gross domestic product (GDP)[62]; hunted mammal richness; distance to strict protected area, based on the World Database on Protected Area; country income group, following World Bank classifications[63]; biogeographic realm[64]; and human population density[65]. All predictors were resampled or aggregated to a common spatial resolution of 5 km to match the spatial resolution of the occurrence dataset. Following collinearity assessment, human population density was excluded from final model fitting, as described in the Supplementary materials (Supplementary Fig. S2).

455

456 Extended Data Table 1. Ecological and anthropogenic predictors used to model the probability of

457 poaching at global scale.

Variable name	Variable description	Rationale
Anthropogenic predictors		
Gross Domestic Product (GDP)	It was obtained from spatially disaggregated estimates at ~10 km resolution, based on the SSP2 scenario. As with population density, annual GDP rasters[62] were downloaded and averaged across the study period to produce a single mean surface.	GDP serves as a proxy for economic development and market capacity for wildlife products. Higher GDP may reflect both greater consumer demand for commercially traded species and the availability of alternative livelihoods that reduce dependence on illegal harvest[34].
Country income group	Countries were classified into five income groups (Low income, Lower-middle income, Upper-middle income, High income OECD and High income non-OECD) according to the World Bank country income classifications (2010)[63]. Each grid cell was assigned the income group of its corresponding country and used as a categorical predictor.	Income groups capture broad socioeconomic differences among countries that may modify the relationship between economic development and poaching pressure[35]. We included an interactive term between GDP and income group to test whether the necessity and motivation to poach differs systematically across income contexts. We hypothesised that in low-income groups, poaching probability would be highest at the lowest GDP

		levels, reflecting subsistence-driven necessity; in middle-income groups, poaching would instead be associated with commercially driven motivations rather than survival need; and in high-income groups, poaching probability would be low across the GDP range, reflecting reduced economic necessity to engage in illegal harvest.
Accessibility to cities	It was measured as motorized travel time in minutes to the nearest urban centre with more than 50,000 inhabitants[60], held constant at 2015 values.	Accessibility to cities captures the logistical feasibility of illegal harvest by reflecting the ease with which hunters can reach wildlife and transport products to market. Areas with shorter travel times to urban centres are expected to experience higher poaching pressure due to lower effort costs and stronger market connectivity[41].
Human population density (persons/km²)	It was obtained from WorldPop v4.0 constrained individual countries estimates at 1 km resolution[65]. Annual rasters were downloaded for the full available period spanning the study extent	Population density represents human hunting pressure and local demand for wildlife products[66]. Excluded from final analyses due to strong collinearity with accessibility

	(2010 to 2020), and a mean raster was computed across all years to produce a single temporally averaged surface representing the characteristic population pressure across the study period.	to cities (Pearson's r = −0.86; see Supplementary)
Distance to roads (km)	It was calculated as the Euclidean distance to the nearest primary or secondary road from the Global Road Inventory Project (GRIP) database[45].	Road proximity determines how easily hunters can access wildlife-rich areas. Areas closer to primary and secondary roads are expected to experience elevated poaching pressure, as roads reduce the time and effort required for illegal harvest[33].
Night-time light intensity (nW cm^{-2} sr^{-1})	It was derived from annual VIIRS day/night band composites[61]. Annual rasters were downloaded and averaged across the study period to produce a single mean surface.	Night-time lights serve as a proxy for human activity intensity and concealment opportunity. While commonly used as a proxy for human footprint in macroecological studies, its specific relationship with poaching occurrence has not been previously quantified at global scale. We hypothesised that poaching preferentially occurs in areas of low illumination where detection risk is reduced, though intermediate light levels, characteristic of the

		rural-urban interface, may also concentrate illegal harvest where accessibility and wildlife availability coincide.
Distance to strict protected areas (km)	It was calculated as the Euclidean distance from each grid cell to the nearest protected area classified as IUCN category I or II in the World Database on Protected Areas (WDPA).	Distance to strict protected areas captures two complementary hypotheses. First, strictly protected areas concentrate enforcement effort, increasing the probability of detecting illegal hunting events and potentially deterring poaching within their boundaries[41]. Second, for species whose populations are now largely confined to protected areas, proximity to PA boundaries may reflect proximity to the last remaining viable populations of target species, making these areas disproportionately attractive to hunters despite, or because of, their protected status[67].
Ecological predictors		
Hunted mammal species richness	It was derived from Area of Habitat (AOH) maps[68] at 100 m resolution, aggregated to 5 km grid cells as the total number of terrestrial mammal species per cell.	Hunted mammal richness represents the diversity and spatial availability of species subject to illegal harvest, providing a more ecologically targeted measure of poaching opportunity than total species

		richness[8]. The derivation of this predictor is described in detail in the Supplementary Methods.
Biogeographic realm	The realms were assigned using the global terrestrial realm classification[64], categorized into seven biogeographic realms (Afrotropical, Palearctic, Indomalayan, Nearctic, Neotropical, Australasian and Oceanic). Each grid cell was assigned to one realm and used as a categorical predictor.	The biogeographic realm captures broad-scale differences in species assemblages and ecological conditions that are likely to modify the relationship between local predictors and poaching occurrence. Hunted mammal richness itself varies substantially across realms, reflecting differences in regional faunal composition and diversity[64]. We therefore included realm as a categorical interaction term to test how the effect of hunted mammal richness on poaching probability varies within each realm, rather than assuming a globally uniform relationship between richness and poaching pressure.

458

459 All continuous predictors exhibiting strong right-skewness (i.e., GDP, accessibility, distance to roads,
460 and night-time light intensity) were $\log_{10}$-transformed after adding a constant of one prior to fitting
461 GAMs. This transformation improved numerical stability and facilitated the estimation of smooth
462 nonlinear relationships. RF models were fitted using the original, untransformed predictor values,
463 as tree-based algorithms are generally insensitive to variable scaling and distributional skewness.

Pseudo-absence selection

Because poaching records consisted of presence-only observations, pseudo-absences were generated to enable binomial model fitting. Pseudo-absence placement is critical, as spatial bias in detection effort can confound estimated environmental relationships[69], and inappropriate environmental placement can influence model discrimination[70]. We therefore employed a two-stage approach that addresses both detection bias and environmental representation.

Stage 1: Detection bias correction. Poaching event detectability likely varies spatially due to heterogeneous monitoring and enforcement effort, with areas of higher patrol intensity or established protected area infrastructure more likely to detect and report incidents. To account for this, we estimated a kernel density estimation (KDE) surface from observed poaching event locations and used it to generate a spatially weighted background pool. Background points were sampled with probabilities proportional to local kernel density values, thereby concentrating sampling in regions with reporting effort broadly comparable to that of observed poaching records and reducing the influence of geographic sampling bias[69].

Stage 2: Environmentally stratified pseudo-absence selection. Pseudo-absences were selected from the KDE-weighted background pool to ensure broad representation of environmental conditions across the study area. This approach avoided excessive concentration of pseudo-absences within a restricted portion of environmental space while maintaining sampling within regions characterised by reporting probabilities comparable to those of observed poaching events. Consequently, pseudo-absences captured the range of environmental conditions represented in the background pool, providing suitable environmental contrast for model calibration.

All pseudo-absences were constrained to be >10 km from any presence point to avoid spatial overlap and reduce misclassification arising from georeferencing imprecision[71,72].
To account for uncertainty associated with pseudo-absence placement, five independent pseudo-absence datasets were generated using different random seeds. Each dataset contained 1,168 pseudo-absence locations, maintaining a 1:1 presence-to-pseudo-absence ratio as recommended for binomial models[70]. All modelling and evaluation procedures were conducted independently for

each replicate, with final metrics and parameter estimates reported as mean ± standard deviation across replicates.

Statistical modelling

Global poaching probability was modelled using two complementary algorithms: Generalized Additive Models (GAMs) and Random Forests (RFs). GAMs provide flexible and interpretable representation of non-linear environmental relationships, whereas RF can accommodate complex interactions and non-linear responses without requiring any prior specification of their functional form, making them complementary to the more parametric GAM framework.

Generalized Additive Models

We fitted GAMs using the R package *mgcv* (v.1.9-4)[73] with a binomial error distribution and logit link function. Predictor effects were modelled using penalized thin-plate regression splines (bs = "tp")[73,74] and smooth terms were fitted with a basis dimension (k = 4), allowing moderate non-linearity while limiting overfitting. However, only distance to protected areas was fitted with k = 2, because preliminary analyses indicated an approximately linear relationship with poaching probability. Smoothness parameters were estimated using Restricted Maximum Likelihood (REML). To allow key predictor effects to vary across ecological and anthropogenic contexts, we modelled interactions between hunted mammal richness and biogeographic realm, and between GDP and income group, using factor-smooth interactions.

Random Forests

RFs were implemented using the R package *ranger*[75] with probability estimation. Hyperparameters were optimized via cross-validated tuning with the tuneRanger[76] package. The tuning procedure explored alternative values of the number of variables considered at each split (mtry), minimum terminal node size (min.node.size), and bootstrap sampling fraction (sample.fraction), selecting the parameter combination that minimized out-of-bag prediction error. Final RF models were subsequently fitted using the optimal parameter configuration identified during tuning.

Model evaluation and cross-validation

Model performance was evaluated using two complementary strategies: conventional random cross-validation and spatial block cross-validation.

527

528 Standard cross-validation

529 For each of the 5 replicate datasets, we conducted conventional 5-fold cross-validation to evaluate
530 overall model discrimination ability. In each fold, the dataset was randomly partitioned into training
531 (80%) and testing (20%) sets. The random partitioning was repeated across five folds with different
532 random splits. This approach evaluates how well models predict held-out data when spatial
533 structure is ignored.

534

535 Spatial block cross-validation

536 Standard random cross-validation can be overly optimistic when data exhibit strong spatial
537 autocorrelation, as training and test data may contain similar environmental conditions and spatial
538 structure. To address this limitation and provide a more realistic assessment of model
539 transferability to genuinely novel geographic areas, we implemented spatial block cross-validation
540 using the *blockCV* package[77]. This method partitions the study area into five geographically distinct,
541 non-overlapping spatial blocks based on spatial clustering. For each fold, one block was withheld for
542 testing while the remaining four blocks were used for model training. This ensures that test data are
543 spatially independent from training data, minimising spatial autocorrelation between training and
544 testing sets and providing a stringent evaluation of whether models can predict poaching
545 probability in geographically distinct regions. Spatial blocks were defined using a range distance of
546 200 km, ensuring sufficient spatial separation between training and test areas.

547

548 Performance metrics

549 For both cross-validation strategies, we evaluated model performance using sensitivity -the
550 proportion of observed poaching locations correctly identified by the model-, and the Boyce index,
551 which evaluates whether predicted suitability values at observed presences are consistently higher
552 than expected under a random distribution. Because the Boyce index does not require true absence
553 data, it is particularly appropriate for evaluating models developed from presence and pseudo-
554 absence datasets. Performance metrics were calculated independently for each pseudo-absence
555 replicate and are reported as mean ± standard deviation across replicates.

556

557 Threshold selection

To convert continuous predicted probabilities into a binary classification of poaching risk for area-based reporting, we selected the threshold that maximised the sum of sensitivity and specificity (maxSSS)[42], calculated from the pooled held-out predictions of the standard 5-fold cross-validation across all five pseudo-absence replicates.

Spatial projection of poaching probability

Final models were used to generate global predictions of poaching occurrence probability across the terrestrial surface. For each of the five pseudo-absence replicates, GAM and RF models were independently refitted on the complete dataset using the predictor specifications and hyperparameter configurations identified during the modelling and tuning procedures described above. Each of the ten models (five GAM and five RF replicates) was then applied to the global predictor raster stack to produce a spatially explicit prediction surface at 5 km resolution. The ensemble mean prediction for each algorithm was computed as the arithmetic mean of the five replicate surfaces, yielding a single representative map of predicted poaching occurrence probability for GAMs and RFs respectively. Spatial uncertainty was quantified as the standard deviation across the five replicate surfaces for each algorithm, reflecting variability in predicted probability attributable to pseudo-absence configuration. To identify grid cells where predictions were generated by extrapolation beyond the environmental conditions represented in the training data, we computed the Multivariate Environmental Similarity Surface (MESS) for each replicate dataset. Grid cells with negative MESS values, indicating environmental conditions not represented in the training data, are considered extrapolation areas and should be interpreted with caution; these are mapped in Supplementary Fig. S5. Both GAM and RF ensemble maps are presented to demonstrate the concordance of predicted spatial patterns across modelling approaches. The GAM is treated as the primary interpretive model, as it provides explicit smooth functions and factor-specific interaction terms that allow direct interpretation of predictor-response relationships. The RF serves as a complementary validation, confirming that the major geographic patterns identified by the GAM are robust to a non-parametric modelling framework that makes no assumptions about functional form. All predictions were constrained to the terrestrial surface excluding Antarctica, and grid cells lacking valid predictor data were excluded from the prediction surface.

Predictor dominance mapping

To identify the locally dominant predictor of poaching risk, we decomposed each GAM's predicted probability into its constituent smooth-term contributions (predict.gam, type = "terms"). For predictors fitted with a realm- or income-specific interaction term (hunted mammal richness, GDP), contributions across factor levels were summed to a single value per cell, since only one level applies at any given location. Term contributions were averaged across the five pseudo-absence replicates, and the predictor with the largest absolute mean contribution was designated as locally dominant for that cell (Fig. 4).

References

1. Ripple, W. J. *et al.* Bushmeat hunting and extinction risk to the world's mammals. *R Soc Open Sci.* **3**, 160498 (2016).
2. Gallego-Zamorano, J. *et al.* Combined effects of land use and hunting on distributions of tropical mammals. *Conserv Biol* **34**, 1271–1280 (2020).
3. Ceballos, G. *et al.* Accelerated modern human–induced species losses: Entering the sixth mass extinction. *Science Advances* **1**, e1400253 (2015).
4. Young, H. S., McCauley, D. J., Galetti, M. & Dirzo, R. Patterns, Causes, and Consequences of Anthropocene Defaunation. *Annual Review of Ecology, Evolution, and Systematics* **47**, 333–358 (2016).
5. Brashares, J. S., Arcese, P. & Sam, M. K. Human demography and reserve size predict wildlife extinction in West Africa. *Proceedings of the Royal Society of London. Series B: Biological Sciences* https://doi.org/10.1098/rspb.2001.1815 (2001) doi:10.1098/rspb.2001.1815.
6. Terborgh, J. and van Schaik, C.P. (1997) Minimizing Species Loss The Imperative of Protection. In Kramer, R., et al., Ed., Protected Areas and the Defense of Tropical Biodiversity, Oxford University Press, New York, 15-35. - References - Scientific Research Publishing. https://www.scirp.org/reference/referencespapers?referenceid=1832372.

7. Duporge, I., Hodgetts, T., Wang, T. & Macdonald, D. W. The spatial distribution of illegal hunting of terrestrial mammals in Sub-Saharan Africa: a systematic map. *Environ Evid* **9**, 15 (2020).
8. Benítez-López, A. *et al.* The impact of hunting on tropical mammal and bird populations. *Science* **356**, 180–183 (2017).
9. Robinson, J. G. & Redford, K. H. Measuring the sustainability of hunting in tropical forests. *Oryx* **28**, 249–256 (1994).
10. *Best Practices in Sustainable Hunting: A Guide to Best Practices from around the World*. (CIC [u.a.], Budakeszi, 2008).
11. Nielsen, M. R., Meilby, H., Smith-Hall, C., Pouliot, M. & Treue, T. The Importance of Wild Meat in the Global South. *Ecological Economics* **146**, 696–705 (2018).
12. Antunes, A. P. *et al.* Healthy forests safeguard traditional wild meat food systems in Amazonia. *Nature* **648**, 625–633 (2025).
13. Wells, G. J. *et al.* Hundreds of millions of people in the tropics need both wild harvests and other forms of economic development for their well-being. *One Earth* **7**, 311–324 (2024).
14. Spencer, D. & Cohen, N. D. Wildlife Poaching in North America: A Systematic Review of Motivations, Opportunity Structures, and Rationalizations. SSRN Scholarly Paper at https://doi.org/10.2139/ssrn.6583487 (2026).
15. Bessone, M. *et al.* Increase in wild animal consumption across Central Africa. *Nature* **653**, 1092–1098 (2026).
16. Morton, O., Scheffers, B. R., Haugaasen, T. & Edwards, D. P. Impacts of wildlife trade on terrestrial biodiversity. *Nat Ecol Evol* **5**, 540–548 (2021).
17. Rija, A. A., Critchlow, R., Thomas, C. D. & Beale, C. M. Global extent and drivers of mammal population declines in protected areas under illegal hunting pressure. *PLOS ONE* **15**, e0227163 (2020).

643 18. Passoni, G., Coulson, T. & Cagnacci, F. Celebrating wildlife population recovery through
644 education. *Trends in Ecology & Evolution* **39**, 101–105 (2024).
645 19. Goboro, E. M., Mbise, F. P. & Ngongolo, K. The Effects of Illegal Wildlife Activities on
646 Biodiversity in Few Selected African Countries. *African Journal of Ecology* **63**, e70055 (2025).
647 20. Moore, J. F. *et al.* What is the effect of poaching activity on wildlife species? *Ecological*
648 *Applications* **31**, e02397 (2021).
649 21. Macdonald, D. W., Boitani, L., Dinerstein, E., Fritz, H. & Wrangham, R. Conserving large
650 mammals. in *Key Topics in Conservation Biology 2* 277–312 (John Wiley & Sons, Ltd, 2013).
651 doi:10.1002/9781118520178.ch16.
652 22. de Souza, J. B. & Alves, R. R. N. Hunting and Wildlife use in an Atlantic Forest Remnant of
653 Northeastern Brazil. *Tropical Conservation Science* **7**, 145–160 (2014).
654 23. Johnson, P., Kansky, R., Loveridge, A. & Macdonald, D. Size, Rarity and Charisma: Valuing
655 African Wildlife Trophies. *PloS one* **5**, e12866 (2010).
656 24. Cardillo, M. *et al.* Multiple Causes of High Extinction Risk in Large Mammal Species. *Science*
657 **309**, 1239–1241 (2005).
658 25. Brodie, J. F., Helmy, O. E., Brockelman, W. Y. & Maron, J. L. Bushmeat poaching reduces the
659 seed dispersal and population growth rate of a mammal-dispersed tree. *Ecological Applications*
660 **19**, 854–863 (2009).
661 26. da Silva Batista, G. *et al.* Defaunation disrupts the behavior of large terrestrial vertebrates,
662 impacting ecological functions in the Amazon. *Global Ecology and Conservation* **59**, e03522
663 (2025).
664 27. Bogoni, J. A., Araujo Goebel, L. G., Santos-Filho, M. & Peres, C. A. Linking functional and
665 phylogenetic diversity to assess decay in ecosystem services induced by metacommunity-level
666 mammal extirpations. *Austral Ecology* **49**, e13597 (2024).
667 28. Lacher, T. E., Jr. *et al.* The functional roles of mammals in ecosystems. *J Mammal* **100**, 942–
668 964 (2019).

669 29. Unit, B. Kunming-Montreal Global Biodiversity Framework. https://www.cbd.int/gbf (2026).
670 30. Venter, O. *et al.* Global terrestrial Human Footprint maps for 1993 and 2009. *Sci Data* **3**,
671 160067 (2016).
672 31. Mu, H. *et al.* A global record of annual terrestrial Human Footprint dataset from 2000 to 2018.
673 *Sci Data* **9**, 176 (2022).
674 32. Gavin, M. C., Solomon, J. N. & Blank, S. G. Measuring and Monitoring Illegal Use of Natural
675 Resources. *Conservation Biology* **24**, 89–100 (2010).
676 33. Espinosa, S., Branch, L. C. & Cueva, R. Road Development and the Geography of Hunting by
677 an Amazonian Indigenous Group: Consequences for Wildlife Conservation. *PLOS ONE* **9**,
678 e114916 (2014).
679 34. Lunstrum, E. & Givá, N. What drives commercial poaching? From poverty to economic
680 inequality. *Biological Conservation* **245**, 108505 (2020).
681 35. Duffy, R., St John, F. A. V., Büscher, B. & Brockington, D. Toward a new understanding of the
682 links between poverty and illegal wildlife hunting. *Conservation Biology* **30**, 14–22 (2016).
683 36. Philippe-Lesaffre, M. *et al.* Mapping hunting probability across the tropics in space and time.
684 *Nat Sustain* 1–11 (2026) doi:10.1038/s41893-026-01924-6.
685 37. Harfoot, M. B. J. *et al.* Using the IUCN Red List to map threats to terrestrial vertebrates at
686 global scale. *Nat Ecol Evol* **5**, 1510–1519 (2021).
687 38. Ferreiro-Arias, I. *et al.* Drivers and spatial patterns of avian defaunation in tropical forests.
688 *Diversity and Distributions* **31**, e13855 (2025).
689 39. Pacifici, M., Cristiano, A., Mancini, G., Nania, D. & Davoli, M. Global hotspots of bushmeat
690 hunting risk for mammals. Preprint at https://doi.org/10.21203/rs.3.rs-6278255/v1 (2025).
691 40. de Matos Dias, D., Ferreguetti, Á. C. & Rodrigues, F. H. G. Using an occupancy approach to
692 identify poaching hotspots in protected areas in a seasonally dry tropical forest. *Biological*
693 *Conservation* **251**, 108796 (2020).

694 41. Ghoddousi, A. *et al.* Understanding spatial patterns of poaching pressure using ranger logbook
695 data to optimize future patrolling strategies. *Ecological Applications* **32**, e2601 (2022).
696 42. Liu, C., White, M. & Newell, G. Selecting thresholds for the prediction of species occurrence
697 with presence-only data. *Journal of Biogeography* **40**, 778–789 (2013).
698 43. Benítez-López, A. *et al.* Defaunation Maps for Tropical Mammals and Birds. *Global Ecology*
699 *and Biogeography* **35**, e70280 (2026).
700 44. Harrison, R. D. Emptying the Forest: Hunting and the Extirpation of Wildlife from Tropical
701 Nature Reserves. *BioScience* **61**, 919–924 (2011).
702 45. Meijer, J. R., Huijbregts, M. A. J., Schotten, K. C. G. J. & Schipper, A. M. Global patterns of
703 current and future road infrastructure. *Environ. Res. Lett.* **13**, 064006 (2018).
704 46. Tan, Y.-L., Yiew, T.-H., Lau, L.-S. & Tan, A.-L. Environmental Kuznets curve for biodiversity
705 loss: evidence from South and Southeast Asian countries. *Environ Sci Pollut Res* **29**, 64004–
706 64021 (2022).
707 47. Velho, N., Karanth, K. K. & Laurance, W. F. Hunting: A serious and understudied threat in
708 India, a globally significant conservation region. *Biological Conservation* **148**, 210–215 (2012).
709 48. Liang, D., Giam, X., Hu, S., Ma, L. & Wilcove, D. S. Assessing the illegal hunting of native
710 wildlife in China. *Nature* **623**, 100–105 (2023).
711 49. Melo-Dias, M. *et al.* Surviving in the Amazon Arc of Deforestation: Richness and Defaunation
712 of Mammals in Priority-Protected Areas of the Brazilian Midwest. *Austral Ecology* **50**, e70088
713 (2025).
714 50. Cezne, E. & Otsuki, K. The Amazon's road to growth? Infrastructural imaginaries of Brazil's
715 BR-319 Highway. *Economy and Society* **54**, 620–646 (2025).
716 51. Musgrave, R. S., Parker, S. & Wolok, M. The Status of Poaching in the United States - Are We
717 Protecting Our Wildlife. *NATURAL RESOURCES JOURNAL* **33**,.

52. Most wildlife crimes in Europe go unpunished or undetected, says a brand-new report. *WWF* https://wwfcee.org/what-we-do/most-wildlife-crimes-in-europe-go-unpunished-or-undetected-says-a-brand-new-report.
53. Bachmann, M. E. *et al.* Analysis of differences and commonalities in wildlife hunting across the Africa-Europe South-North gradient. *PLOS Biology* **20**, e3001707 (2022).
54. Jung, M. *et al.* Areas of global importance for conserving terrestrial biodiversity, carbon and water. *Nat Ecol Evol* **5**, 1499–1509 (2021).
55. Hauenstein, S., Kshatriya, M., Blanc, J., Dormann, C. F. & Beale, C. M. African elephant poaching rates correlate with local poverty, national corruption and global ivory price. *Nat Commun* **10**, 2242 (2019).
56. wildlifetradeportal.org/dashboard. https://www.wildlifetradeportal.org/dashboard.
57. Welcome to CLT. *Cape Leopard Trust, South Africa* https://capeleopard.org.za/.
58. Zhao, Z.-X., Shao, M.-L., Newman, C., Luo, Y. & Zhou, Z.-M. Species availability and socio-economics drive prosecutions for regional mammal and bird poaching across China, 2014–2020. *Global Ecology and Conservation* **46**, e02583 (2023).
59. Critchlow, R. *et al.* Improving Law-Enforcement Effectiveness and Efficiency in Protected Areas Using Ranger-collected Monitoring Data. *Conservation Letters* **10**, 572–580 (2017).
60. Weiss, D. J. *et al.* A global map of travel time to cities to assess inequalities in accessibility in 2015. *Nature* **553**, 333–336 (2018).
61. Elvidge, C. D., Baugh, K., Zhizhin, M., Hsu, F. C. & Ghosh, T. VIIRS night-time lights. *International Journal of Remote Sensing* **38**, 5860–5879 (2017).
62. Murakami, D., Yoshida, T. & Yamagata, Y. Gridded GDP Projections Compatible With the Five SSPs (Shared Socioeconomic Pathways). *Front. Built Environ.* **7**, (2021).
63. Understanding country income: World Bank Group income classifications for FY26. *World Bank Blogs* https://blogs.worldbank.org/en/opendata/understanding-country-income--world-bank-group-income-classifica.

64. Olson, D. M. *et al.* Terrestrial Ecoregions of the World: A New Map of Life on Earth: A new global map of terrestrial ecoregions provides an innovative tool for conserving biodiversity. *BioScience* **51**, 933–938 (2001).
65. Tatem, A. J. WorldPop, open data for spatial demography. *Sci Data* **4**, 170004 (2017).
66. Fa, J. E., Peres, C. A. & Meeuwig, J. Bushmeat Exploitation in Tropical Forests: an Intercontinental Comparison. *Conservation Biology* **16**, 232–237 (2002).
67. Pacifici, M., Di Marco, M. & Watson, J. E. M. Protected areas are now the last strongholds for many imperiled mammal species. *Conservation Letters* **13**, e12748 (2020).
68. Lumbierres, M. *et al.* Area of Habitat maps for the world's terrestrial birds and mammals. *Sci Data* **9**, 749 (2022).
69. Phillips, S. J. *et al.* Sample selection bias and presence-only distribution models: implications for background and pseudo-absence data. *Ecological Applications* **19**, 181–197 (2009).
70. Barbet-Massin, M., Jiguet, F., Albert, C. H. & Thuiller, W. Selecting pseudo-absences for species distribution models: how, where and how many? *Methods in Ecology and Evolution* **3**, 327–338 (2012).
71. VanDerWal, J., Shoo, L. P., Johnson, C. N. & Williams, S. E. Abundance and the Environmental Niche: Environmental Suitability Estimated from Niche Models Predicts the Upper Limit of Local Abundance. *The American Naturalist* **174**, 282–291 (2009).
72. Senay, S. D., Worner, S. P. & Ikeda, T. Novel Three-Step Pseudo-Absence Selection Technique for Improved Species Distribution Modelling. *PLOS ONE* **8**, e71218 (2013).
73. Wood, S. N. *Generalized Additive Models: An Introduction with R, Second Edition*. (Chapman and Hall/CRC, New York, 2017). doi:10.1201/9781315370279.
74. Wood, S. N. Thin Plate Regression Splines. *J. R. Stat. Soc. Ser. B. Stat. Methodol.* **65**, 95–114 (2003).
75. Wright, M. N. & Ziegler, A. ranger: A Fast Implementation of Random Forests for High Dimensional Data in C++ and R. *Journal of Statistical Software* **77**, 1–17 (2017).

76. Probst, P., Wright, M. N. & Boulesteix, A.-L. Hyperparameters and tuning strategies for random forest. *WIREs Data Mining and Knowledge Discovery* **9**, e1301 (2019).
77. Valavi, R., Elith, J., Lahoz-Monfort, J. J. & Guillera-Arroita, G. blockCV: An r package for generating spatially or environmentally separated folds for k-fold cross-validation of species distribution models. *Methods in Ecology and Evolution* **10**, 225–232 (2019).

Supplementary Files

This is a list of supplementary files associated with this preprint. Click to download.

- SupplementaryInformation.pdf